PRELIMINARY FOREST TREE SPECIES CLASSIFICATION IN NORTHERN PROVINCES OF MONGOLIA USING SENTINEL-2 AND MACHINE LEARNING APPROACH

Erdenetuya Boldbaatar , Piotr Wężyk , Wojciech Krawczyk

Department of Forest Resources Management, Faculty of Forestry, University of Agriculture in Krakow, Krakow, Poland

Manuscript received: September 19, 2025
Revised version: November 12, 2025

Boldbaatar E., Wężyk P., Krawczyk W., 2026. Preliminary forest tree species classification in northern provinces of Mongolia using Sentinel-2 and machine learning approach. *Quaestiones Geographicae* 45(1), Bogucki Wydawnictwo Naukowe, Poznań, pp. 139–154. 11 figs, 5 tables.

Abstract: This research addresses the need for precise, wide-scale monitoring of Mongolia's boreal forests, as a part of a critical ecosystem that stores nearly 30% of global terrestrial carbon. Covering approximately 7.37 Mha in Mongolia, these forests form the southern fringe of the Siberian taiga and are increasingly affected by wildfires (95.9% of total forest losses) and logging (2.5% of losses) since 2000. The study focuses on Selenge, Darkhan-Uul and Tuv provinces located in northern Mongolia, where traditional forest inventory methods do not work well due to the extensive and difficult or inaccessible terrain. To overcome these challenges and needs of precise forest monitoring, we developed a classification framework using Sentinel-2 (European Space Agency [ESA]) multi-temporal satellite imageries (period 2020–2024), acquiring key phenological stages. We applied a random forest (RF) algorithm to classify five dominant tree species, that is, Siberian pine (SBP) (*Pinus sibirica* Ledeb.), Scotch pine (SP) (*Pinus sylvestris* L.), Siberian Larch (SBL) (*Larix sibirica* Ledeb.), Siberian spruce (SBS) (*Picea obovata* Ledeb.) and Manchurian birch (MB) (*Betula platyphylla* Sukaczev), forming the forest stand cover. The results of Sentinel-2 imageries processing demonstrate very high classification overall accuracy (OA = 96.19%, κ = 0.949). Compared with existing forest management maps (based on *in situ* surveys), SBS (*P. obovata* Ledeb.) area share was underestimated, whereas MB (*B. platyphylla*) area share was overestimated, indicating observable differences in traditional forest inventories. This Sentinel-2 classification approach offers timely, cost-effective and accurate data tailored to Mongolian conditions, supporting sustainable forest management, conservation, reforestation, afforestation and REDD + programmes (Reducing Emissions from Deforestation and Forest Degradation).

Keywords: random forest, Sentinel-2 classification, spectral-multi-temporal analyses, tree species discrimination, Northern Mongolia

Corresponding author: Erdenetuya Boldbaatar; erdenetuya.boldbaatar@student.urk.edu.pl

Introduction

Boreal forests, also known as the taiga, are among the most extensive and ecologically vital terrestrial biomes on Earth, spanning approximately 1.89 billion ha globally and representing nearly one-third of the world's forest cover (UNECE 2024). These forests play a central role in regulating the global climate by storing vast amounts of carbon, influencing hydrological cycles and providing critical habitats for a wide range of flora and fauna adapted to high-latitude,

https://doi.org/10.14746/quageo-2026-0009
ISSN 2082-2103, eISSN 2081-6383

cold environments (Keenan 2015, Senez-Gagnon et al. 2018).

Geographically, boreal forests form a belt across the northern hemisphere, extending from Alaska through Canada, northern Europe, Russia and into parts of northern Mongolia and northeastern China. In Mongolia, these forests primarily occur in the northern and northeastern provinces, such as Selenge, Khentii, Khuvsgul, Bulgan and Zavkhan, covering around 7.37 Mha, that is approximately 8% of the entire country (Ecological Connectivity of Forest Ecosystems 2025, Global forest watch 2024). The Mongolian northern forests are dominated by species such as Siberian larch (SBL) (*Larix sibirica* Ledeb.) (74.3%), Scotch pine (SP) (*Pinus sylvestris* L.) (5.1%), Siberian pine (SBP) (*Pinus sibirica* Ledeb.) (6.2%) and Manchurian birch (MB) (*Betula platyphylla* Sukaczev) (12.1%), which form coniferous, deciduous and mixed-forest stands (Dulamsuren et al. 2010a, b, Ochirbat et al. 2022).

These forests safeguard soil and water, store carbon, conserve biodiversity and sustain livelihoods. In the last decades, Mongolia's boreal forests have faced increasing degradation due to both anthropogenic pressures and natural disasters. Between 2001 and 2024, Mongolia lost around 439,000 ha of forest, which equates to a 11% decrease in wooded areas since 2000. Wildfires were the primary driver (95.9%), followed by logging (2.5%) and other forest disturbances. Since 2000, the Selenge Province, a key forested area, have experienced the highest forest loss (141,000 ha) but at the same time the largest gains (37,100 ha) due to reforestation and natural regeneration, where observed (Global forest watch 2024).

Discrepancies in national and international forest statistics complicate efforts to track and manage forest changes. Global forest watch (2024) estimates Mongolia's forested area at 7.37 Mha, whereas FAO's Global Forest Resources Assessment (2021) reports 14.1 Mha and the National Statistics Office of Mongolia (2025) reports only 12.1 Mha. Mongolia's remaining forest resources, including the arid and semi-arid sago saxaul (*Haloxylon ammodendron* C. A. Mey.), are composed of drought-tolerant species and are almost entirely state-owned, with approximately 100% of Mongolia's forests classified as State Forests (Ministry of Environment and Green Development of Mongolia 2015).

Significant discrepancies in forest cover in Mongolia result from differing definitions (e.g. canopy cover and tree height), methodological approaches (satellite vs. field surveys) and reporting intervals (Hansen et al. 2013, National Statistic office of Mongolia 2025, United Nations 2015). In Mongolia, the recent systematic adoption of advanced remote sensing techniques further challenges data comparability (Silva et al. 2022). This underscores the urgent need for a standardised, transparent monitoring framework to establish a consistent baseline to monitor forest resources in Mongolia.

In addition, over the past two decades, Mongolia's mean annual temperature has increased by approximately 2.1°C, contributing to a rise in environmental hazards such as wildfires, with more than 1400 incidents reported annually. In response to this crisis, the Mongolian government launched the 'One Billion Tree' campaign in 2021 to mitigate climate change through large-scale reforestation (Galtbayar et al. 2022, Ministry of Environment and Tourism 2021).

Addressing these data inconsistencies and improving forest monitoring capabilities are crucial, and recent advances in remote sensing and machine learning (ML) have emerged as vital tools, offering promising solutions for more accurate and large-scale forest classification and management. Advances in satellite imaging technology, particularly the European Space Agency's (ESA) Sentinel-2 (A, B and C) mission, offer relatively high-resolution (HR) multispectral data capable of capturing and monitoring forest phenology and species-level differences. Globally, ML algorithms such as random forest (RF), support vector machines (SVM) and convolutional neural networks (CNN) have demonstrated high accuracy in forest mapping (Grabska-Szwagrzyk and Tymińska-Czabańska 2024, Immitzer et al. 2016, Persson et al. 2018). For example, studies in Germany and Poland have successfully used multi-temporal Sentinel-2 (ESA) imageries combined with national forest inventories to classify more than 10 main tree species with accuracies >80% (Blickensdörfer et al. 2024).

In the past, Amarsaikhan et al. (2012) utilised Landsat (NASA) and ALOS PALSAR data to classify forest areas in northern Mongolia, achieving classification accuracy of 90.78%. Erdenebaatar and Damdinsuren (2020) used object-based

classification (GEOBIA) on Sentinel-2 imagery in Bogdkhan Mountain, reporting 90.87% accuracy. Norovsuren et al. (2023) developed the Spectral Forest Index (SFI) from Sentinel-2, aligning well with ground inventory data. Based on these principles, this study aims to develop and rigorously test a classification framework using multi-temporal Sentinel-2 (ESA) imageries with a RF classifier of the forest cover in the Mandal, Yruu, Khuder (sub-province of Selenge), Khongor, Shariin gol (sub-province of Darkhan-Uul), a key region for both events, such as forest loss and forest recovery in Mongolia.

In this study, we address the primary research questions as follows:

- What is the classification accuracy of dominant tree species in the northern part of Mongolia using multi-temporal Sentinel-2 (ESA) series of satellite imageries and a RF classifier?
- Is it possible to detect changes in the forest tree species composition based on the classification performed on the multi-temporal Sentinel-2 imagery?
- What are the limitations of the remote sensing based on tree species classification approach?

Study area

The study focuses on a sub-province, Mandal, Bayangol, Javkhlant, Yruu, Khuder in Selenge Province and Khongor, Shariin gol sub-province in Darkhan-Uul Province, and Erdene sub-province in Tuv Province, northern Mongolia (48°51'14"N; 106°27'31"E), approximately 300 km north of Ulaanbaatar (Fig. 1). The test area lies at 7386.27 km^2 within the southern extent of the Siberian boreal taiga forest biome, forming a transitional ecotone between forest and steppe. It is characterised by high ecological heterogeneity due to complex topography, continental climate and varied types of vegetation (Dulamsuren et al. 2010a, b).

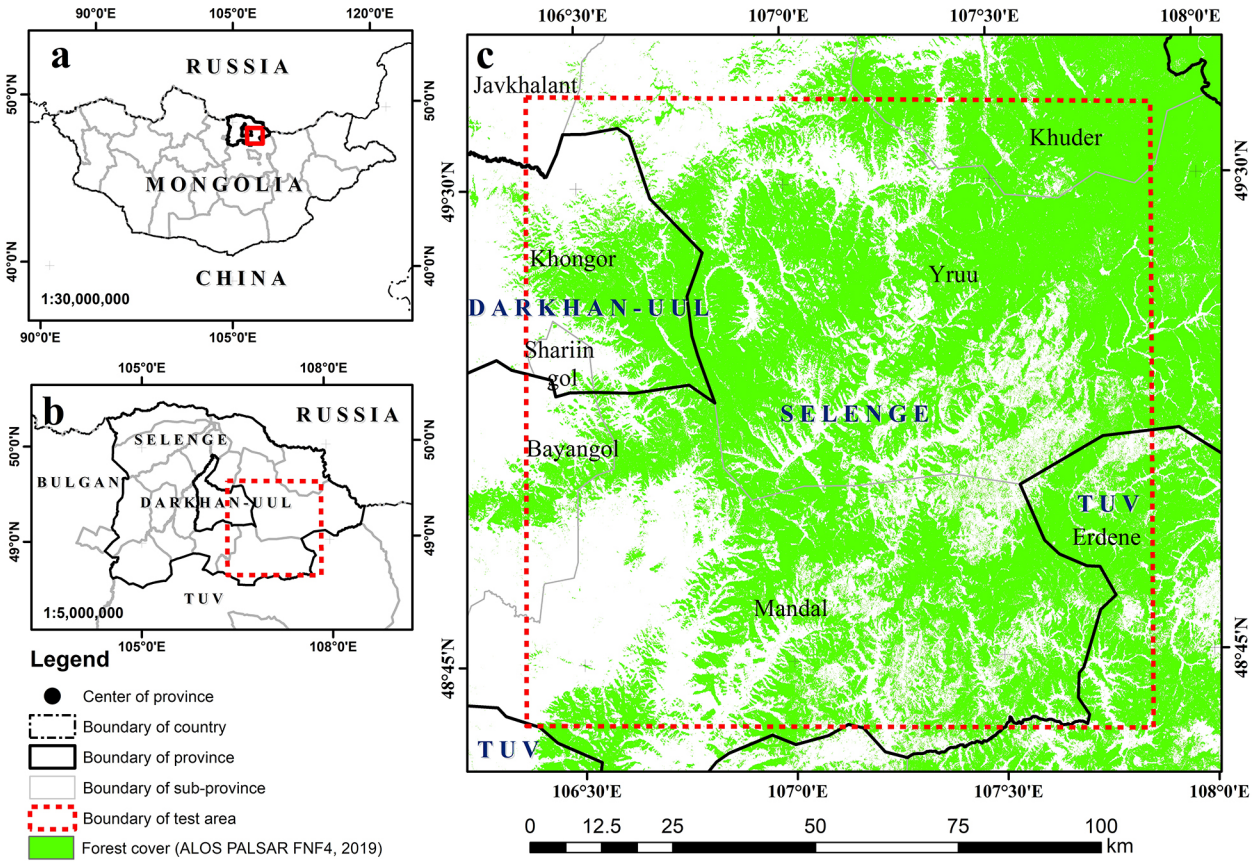

Fig. 1. Study area: (A) Overview map; (B) Provinces in test area: Selenge, Darkhan-Uul and Tuv; (C) Test area over sub-provinces: Mandal, Bayangol, Javkhlant, Yruu, Khuder, Khongor, Shariin gol and Erdene (Mongolian Environmental Database, 2025).

The Selenge, Darkhan-Uul and Tuv Provinces span 11.6 Mha, of which 13.4% is forested (Global forest watch 2024). Dominant tree species includes SP (P. sylvestris, share of 28.9%), birch (*Betula* spp., 27%), SBL (L. sibirica, 25.9%), SBP (*P. sibirica*, 15.2%) and Siberian spruce (SBS) (*Picea obovata*, 0.7%; Environmental Information Center 2025) (Fig. 2). The dominant forest soils in the study area are Podzols, Kastanozems-Chernozems-Phaeozems and Cambisols type (Jugder et al. 2018).

The elevation range is from 700 m to 1600 m above sea level (a.s.l.). It experiences a continental climate with mean annual temperatures from −4°C to +2°C and annual precipitation of 250–400 mm, most common between June and August (Dulamsuren et al. 2010a, b). In Selenge Darkhan-Uul and Tuv provinces between 2001 and 2024, wildfires were responsible for 96% of tree cover loss in the region (Fig. 3), making them the dominant disturbance factor (Global forest watch 2024). In contrast, between 2000 and 2020, the province experienced a 40,018 ha increase in forested area, accounting for 51% of Mongolia's total forest restoration during that period.

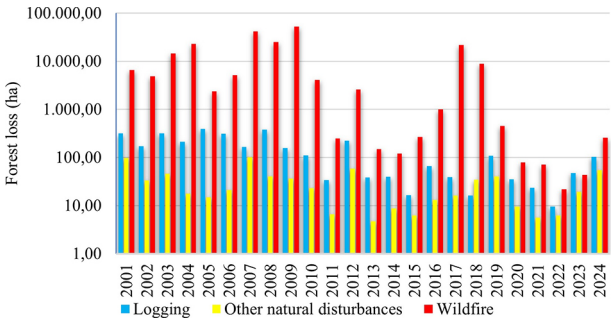

Fig. 3. Main drivers of forest loss in Selenge, Darkhan-Uul and Tuv provinces (2001–2024).

Materials and methods

The methodological concept of this study is based on a supervised ML framework integrating multi-temporal Sentinel-2 imagery and the

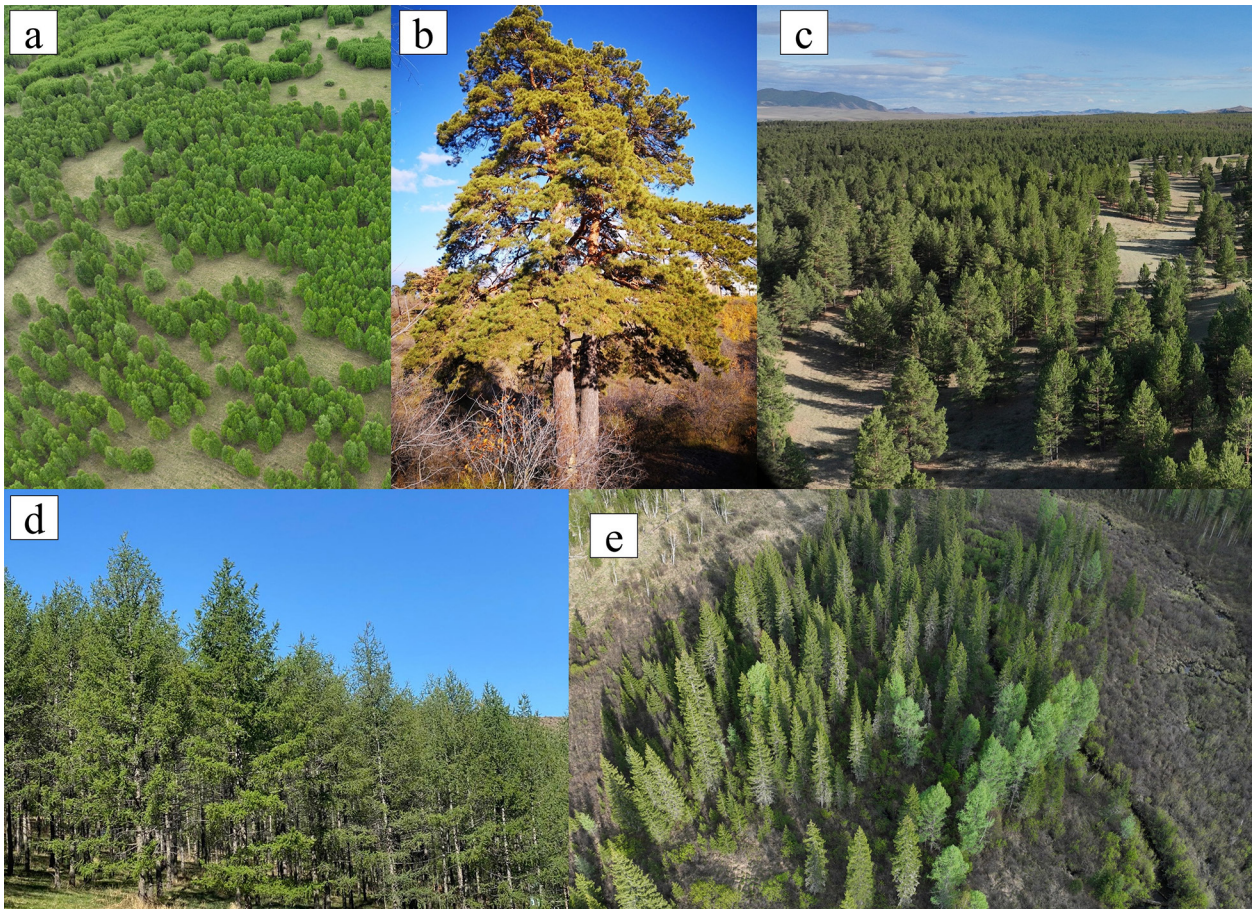

Fig. 2. Examples of dominant tree species in northern Mongolia: (A) MB; (B) SBL; (C) SP; (D) SBP; (E) SBS. MB, Manchurian birch; SBL, Siberian larch; SBP, Siberian pine; SBS, Siberian spruce; SP, Scotch pine.

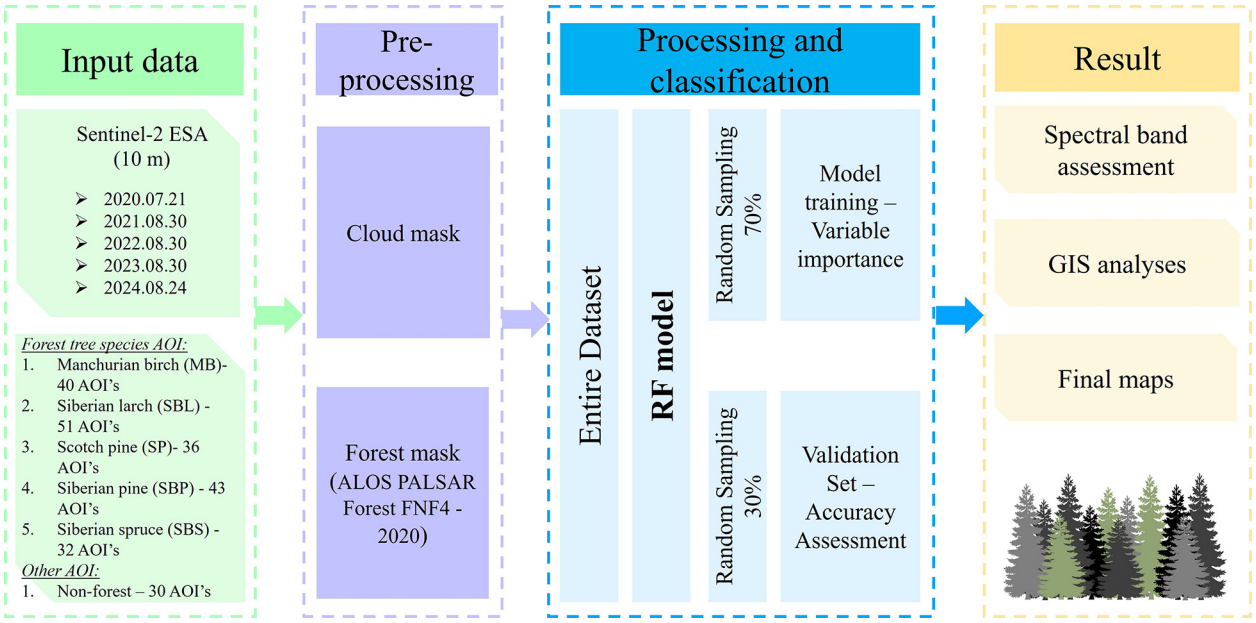

Fig. 4. Flow chart of data processing.

RF classifier for forest tree species discrimination (Fig. 4). The workflow was designed to ensure reproducibility, scalability and statistical robustness of species mapping across heterogeneous boreal landscapes in northern Mongolia. The RF algorithm was chosen for its demonstrated reliability and accuracy in remote sensing-based ecological classification tasks (Belgiu and Drăgu 2016, Grabska-Szwagrzyk and Tymińska-Czabańska 2024, Maxwell et al. 2018).

Data

This study utilised satellite-based data sources to develop and validate the forest tree species classification framework. These datasets were selected to ensure comprehensive spatial, spectral and temporal coverage, as well as high-quality reference information.

Satellite imagery – Sentinel 2 ESA

We utilised five Sentinel-2 (Level 2A; ESA) surface reflectance imageries acquired between 2020 and 2024. The Sentinel-2 constellation (S-2A, S-2B and S-2C) offers 13 spectral bands at 10–60 m GSD (Ground Sampling Distance) with a 5-day revisit cycle (Drusch et al. 2012). A total of nine Sentinel-2 (S-2) cloud-free scenes (<10% cloud cover) were selected across five growing seasons (i.e. July–August): 21 July 2020; 30 August 2021; 30 August 2022; 30 August 2023 and 24 August 2024. These HR satellite images were used to build a consistent dataset covering the 7386.27 km² study area (ESA 2024) (Fig. 5).

The analysed periods (July–August) were strategically chosen to coincide with the peak of the growing season in the boreal forests of northern Mongolia. These periods are characterised by maximal leaf-area development and photosynthetic activity, which maximises the spectral separability between coniferous and deciduous species (e.g. the high reflectance of MB in the near-infrared [NIR] spectrum). Furthermore, this time frame typically experiences minimal cloud cover, a critical practical consideration for obtaining a cloud-free, multi-temporal satellite image.

Reference data

For the S-2 (ESA) RF image classification, we planned to use polygons (area of interest [AOI]) derived from the Mongolian Forest Inventory (2019), provided by the General Authority for Forestry and the Environment in Mongolia (Fig. 6). This dataset included compartment-level attributes such as dominant tree species, forest stand age, canopy cover and disturbance history. Only homogeneous, single-species forest stands were selected and used in this study. The AOIs represented five dominant boreal species: MB (*B. platyphylla* Sukaczev; MB), SBL (*L. sibirica*

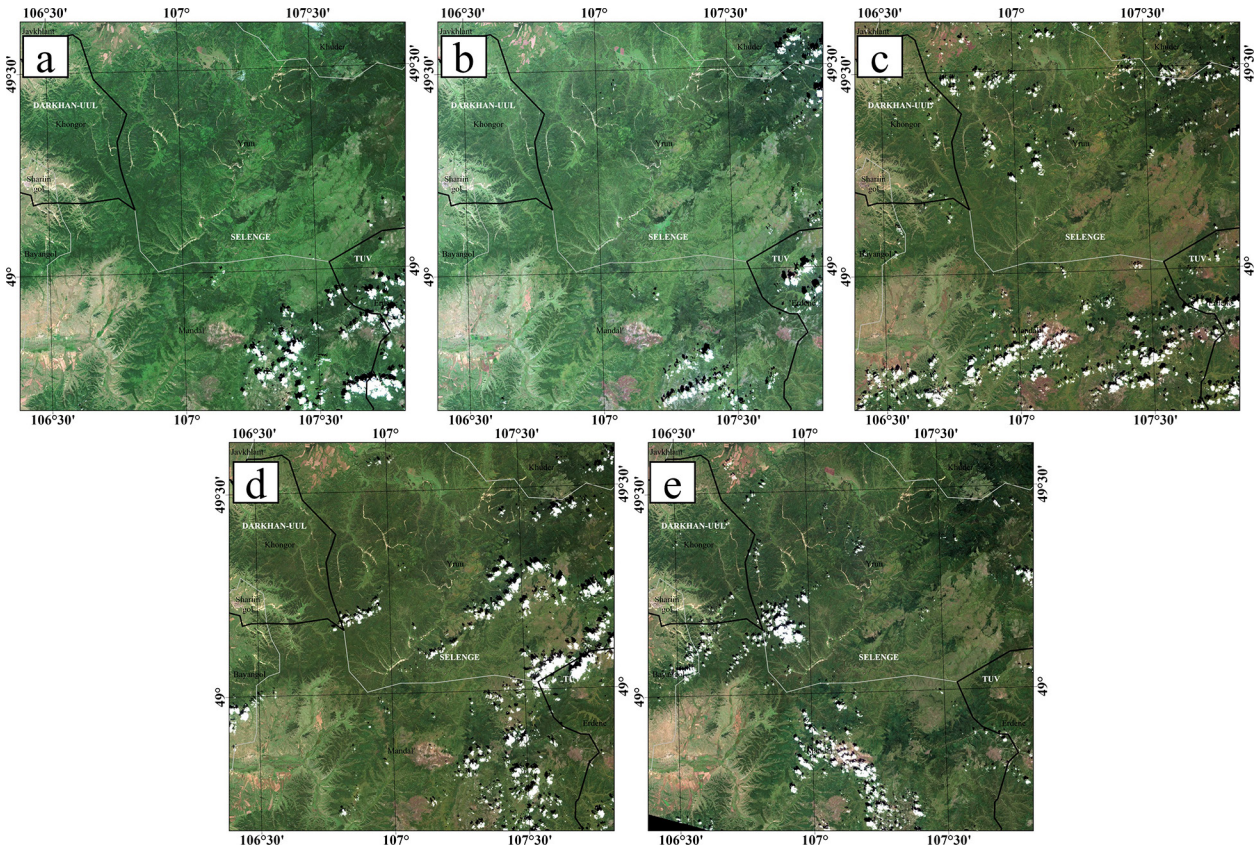

Fig. 5. The Sentinel-2A (ESA) imageries during LEAF-ON (Leaf-on growing season) period used in the study: (A) 21.07.2020; (B) 30.08.2021; (C) 30.08.2022; (D) 30.08.2023; (E) 24.08.2024. ESA, European Space Agency.

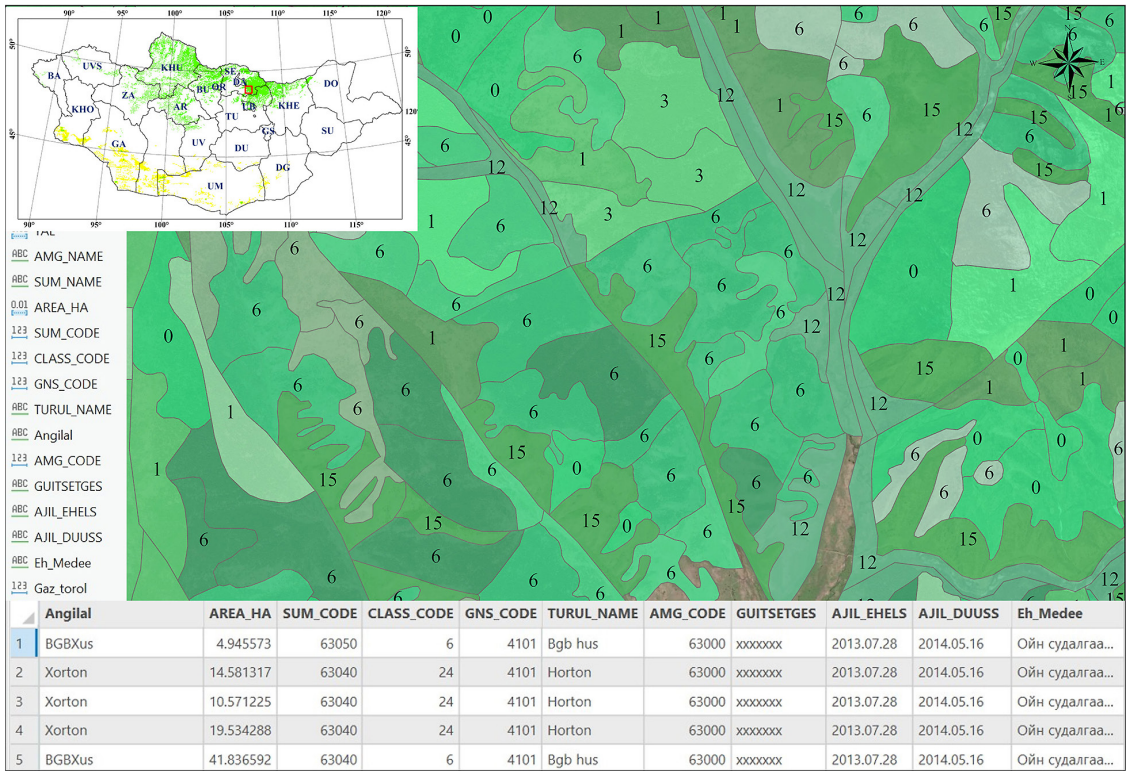

	Angilal	AREA_HA	SUM_CODE	CLASS_CODE	GNS_CODE	TURUL_NAME	AMG_CODE	GUITSETGES	AJIL_EHELS	AJIL_DUUSS	Eh_Medee
1	BGBXus	4.945573	63050	6	4101	Bgb hus	63000	xxxxxxx	2013.07.28	2014.05.16	Ойн судалгаа...
2	Xorton	14.581317	63040	24	4101	Horton	63000	xxxxxxx	2013.07.28	2014.05.16	Ойн судалгаа...
3	Xorton	10.571225	63040	24	4101	Horton	63000	xxxxxxx	2013.07.28	2014.05.16	Ойн судалгаа...
4	Xorton	19.534288	63040	24	4101	Horton	63000	xxxxxxx	2013.07.28	2014.05.16	Ойн судалгаа...
5	BGBXus	41.836592	63040	6	4101	Bgb hus	63000	xxxxxxx	2013.07.28	2014.05.16	Ойн судалгаа...

Fig. 6. Example of the Mongolian forest digital forest map containing data form field inventory visualised in ArcGIS Pro software (Esri, Redlands, CA, USA) (Data source: Mongolian Agency of Forestry 2019).

Ledeb.; SBL), SP (*P. sylvestris* L.; SP), SBP (*P. sibirica* Ledeb.; SBP) and SBS (*P. obovata* Ledeb.; SBS), stratified to ensure ecological representativeness.

The AOIs were initially extracted from the Mongolian digital forest inventory map. Their boundaries were then manually refined through on-screen digitisation using a S-2 false-colour infrared (CIR) composite generated from the Red, Green, and NIR bands (10 m GSD). This specific band combination maximises the spectral contrast between forested and non-forested areas, enabling precise manual delineation (Table 1).

The statistical characteristics of the finalised AOIs are summarised in Table 1. A total of 202 forested AOIs were utilised, spanning a combined area of 2231.0 ha. The number of samples per species ranged from 32 (*P. obovata* Ledeb.) to 51 (*L. sibirica* Ledeb.), reflecting both the relative abundance of species in the region and the need to ensure a minimum sample size for minority classes. The mean area of individual AOIs was 11.04 ha, with species-specific means ranging from 5.25 ha (*P. obovata* Ledeb.) to 15.51 ha (*P. sibirica* Ledeb.). This variation is attributable to the natural patch size distribution of the species and the challenge of delineating large, homogeneous stands for less common species like spruce.

The AOIs were split into training (70%) and validation (30%) subsets using spatial stratified sampling to minimise spatial autocorrelation (Lechner et al. 2020). This resulted in a robust dataset for model training and a statistically independent set for accuracy assessment.

Mean NDVI (Normalized Difference Vegetation Index) values for the analysed tree species AOIs are presented in Figure 7, where the graph

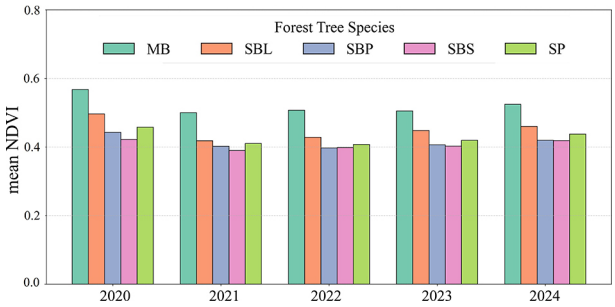

Fig. 7. Mean NDVI values of AOIs of analysed tree species in test site. AOIs, area of interest.

aims to demonstrate the spectral-temporal differences between the five tree species. MB (*B. platyphylla* Sukaczev) consistently had the highest mean NDVI values (0.50–0.57) across 2020–2024 compared to the other tree species. In contrast, SBL (*L. sibirica* Ledeb.), SBP (*P. sibirica* Ledeb.) and SBS (*P. obovata* Ledeb.) maintained lower and relatively stable NDVI values around 0.39–0.46 throughout the study period.

While the consistent NDVI difference between deciduous and coniferous species demonstrates the potential for further species classification, the minimal contrast between conifers, particularly between SBP (*P. sibirica* Ledeb.) and SBS (*P. obovata* Ledeb.), may pose a challenge for accurate classification.

Data processing

Satellite data acquisition and pre-processing

Atmospherically corrected Sentinel-2 (Level 2A) imageries were selected based on seasonal vegetation phenology and low percentage of cloud cover. Only S-2 11 bands with 10, 20 and 60 m GSD were retained. The 20 m and 60 m GSD

Table 1. Basic statistic for area of interest (AOI).

No.	Class	Number of AOI (pcs)	Min AOI area (ha)	Mean AOI area (ha)	Max AOI area (ha)	Total AOI area (ha)	Percentage of total samples (%)
Land use and land cover forest: Tree species							
1	Manchurian birch (*B. platyphylla* Sukaczev)	40	0.3	12	47.6	494	17.2
2	Siberian larch (*L. sibirica* Ledeb.)	51	0.3	8	49.5	388	22.0
3	Scotch pine (*P. sylvestris* L.)	36	2.7	14	57.1	514	15.5
4	Siberian pine (*P. sibirica* Ledeb.)	43	0.3	16	84.6	667	18.5
5	Siberian spruce (*P. obovata* Ledeb.)	32	0.7	5	28.3	168	13.8
Other land use and land cover classes							
1	Non-forest	30	0.1	9	59.4	314	12.9

bands were resampled to 10 m GSD using bilinear interpolation to ensure consistency for pixel-based classification. S-2 spectral bands were scaled by dividing Digital Numbers (DNs) by 10,000 to obtain top-of-canopy reflectance, following ESA standards (Drusch et al. 2012). The final band stack included B1 (Coastal), B2 (Blue), B3 (Green) and B4 (Red); B5 (Red Edge 1), B6 (Red Edge 2) and B7 (Red Edge 3); B8 (NIR), B8A (Red Edge 4), B11 (SWIR 2) and B12 (SWIR 3).

Initially, all pixels affected by clouds and cloud shadows within the S-2 imagery were identified and delineated. A corresponding vector mask was generated and applied to remove these areas. Subsequently, a forest cover mask was derived from the Global 4-class PALSAR-2/PALSAR Forest/Non-Forest (FNF4) dataset, accessed via Google Earth Engine (GEE). Each S-2 raster was first corrected using the cloud-free mask and then spatially constrained using the forest cover mask, thereby isolating exclusively forested regions. This sequential masking approach ensured the derivation of a spatially coherent dataset, comprising only cloud-free forested areas, suitable for subsequent classification and remote sensing analyses.

Feature extraction

Vector-based training data sets (AOIs) were rasterised to ensure spatial congruence with S-2 imagery at a 10 m GSD, thereby facilitating compatibility with pixel-based classification methods. From these rasterised AOIs, representative samples were extracted to obtain per-pixel spectral reflectance values across all used spectral bands. This process yielded a structured dataset comprising spectral bands as predictor variables and corresponding forest tree species classes as response labels, suitable for supervised classification. This methodological workflow is consistent with established remote sensing practices for generating image-aligned training datasets (Lechner et al. 2020) (Fig. 4).

In total, 222,870 samples were extracted, comprising 156,012 training (70%) and 66,858 testing (30%) samples. Forest classes represented 94.9% of all samples, while non-forest areas accounted for 5.1% (Table 2).

RF classification

The RF algorithm (Breiman 2001) was used to classify forest cover and identify the dominant forest tree species in the test area. The RF algorithm was selected due to its proven effectiveness in handling high-dimensional and heterogeneous remote sensing data, as well as its reliability against overfitting (Belgiu and Drăgu 2016). The model's performance was assessed using the out-of-bag (OOB) error estimate, which provides an unbiased measure of generalisation error by evaluating each tree on the data not included in its bootstrap sample. Additionally, the number of variables considered at each *split* (mtry) was optimised using 10-fold *k*-value cross-validation, selecting the optimal mtry value from [2, 4, 6, 8, 10, 12] to enhance classification accuracy (Ming et al. 2016). The number of trees parameter was held at a constant value of 500.

Although mean NDVI values were calculated and analysed to illustrate the spectral-temporal variability between tree species (Fig. 7), NDVI was not included as an input feature in the RF classification model. The RF algorithm utilised only Sentinel-2 spectral bands (B1–B12) as predictor variables. This decision aimed to evaluate the model's capacity to distinguish tree species directly from spectral reflectance data without vegetation indices.

Table 2. Number of S2 rasters (10 m GSD) used for training and testing in random forest classification (bold values represent the total area and overall percentage across all classes).

Classification		Training samples (train)	Testing samples (test)	Total	Overall percentage (%)
LULC forest: Tree species					
1	Manchurian birch	34,132	14,627	48,759	21.9
2	Siberian larch	26,313	11,277	37,590	16.9
3	Scotch pine	35,723	15,309	51,032	22.9
4	Siberian pine	40,829	17,497	58,326	26.2
5	Siberian spruce	11,066	4742	15,808	7.1
Other LULC classes					
1	Non-forest	7949	3406	11,355	5.1
	Total	156,012	66,858	22,287	100.0

Field validation and accuracy assessment

The training set AOIs were proportionally distributed across all defined classes to ensure adequate representation of their variability.

For the accuracy assessment of S-2 classification performance, an error matrix (confusion matrix) was computed based on the predicted and reference class labels from the test AOI set. From this matrix, standard accuracy metrics were derived, including OA, which quantifies the proportion of correctly classified pixels across all categories. Additional metrics, such as the Cohen's kappa coefficient, were also calculated to provide a more comprehensive evaluation of class-specific performance and overall agreement beyond chance.

OA:

$$\mathrm{OA} = \frac{\sum_i n_{ii}}{N} \tag{1}$$

where:

- n_{ii} is the number of correct predictions for class *i*.

These are the diagonal elements of the confusion matrix, representing where the predicted class matches the true class and N is the total number of samples (Congalton 2019):

Cohen's kappa (κ):

$$\kappa = \frac{P_0 - P_e}{1 - P_e} \tag{2}$$

where:

- P_o is observed agreement,
- P_e is expected by chance.

Statistics derived from the confusion matrix were used to assess the reliability of the classification model.

Results

Temporal dynamics of forest tree species classification (2020–2024)

The results of forest tree species classification based on S-2 satellite imagery from 2020 to 2024 in individual tree species within the study area (Fig. 8).

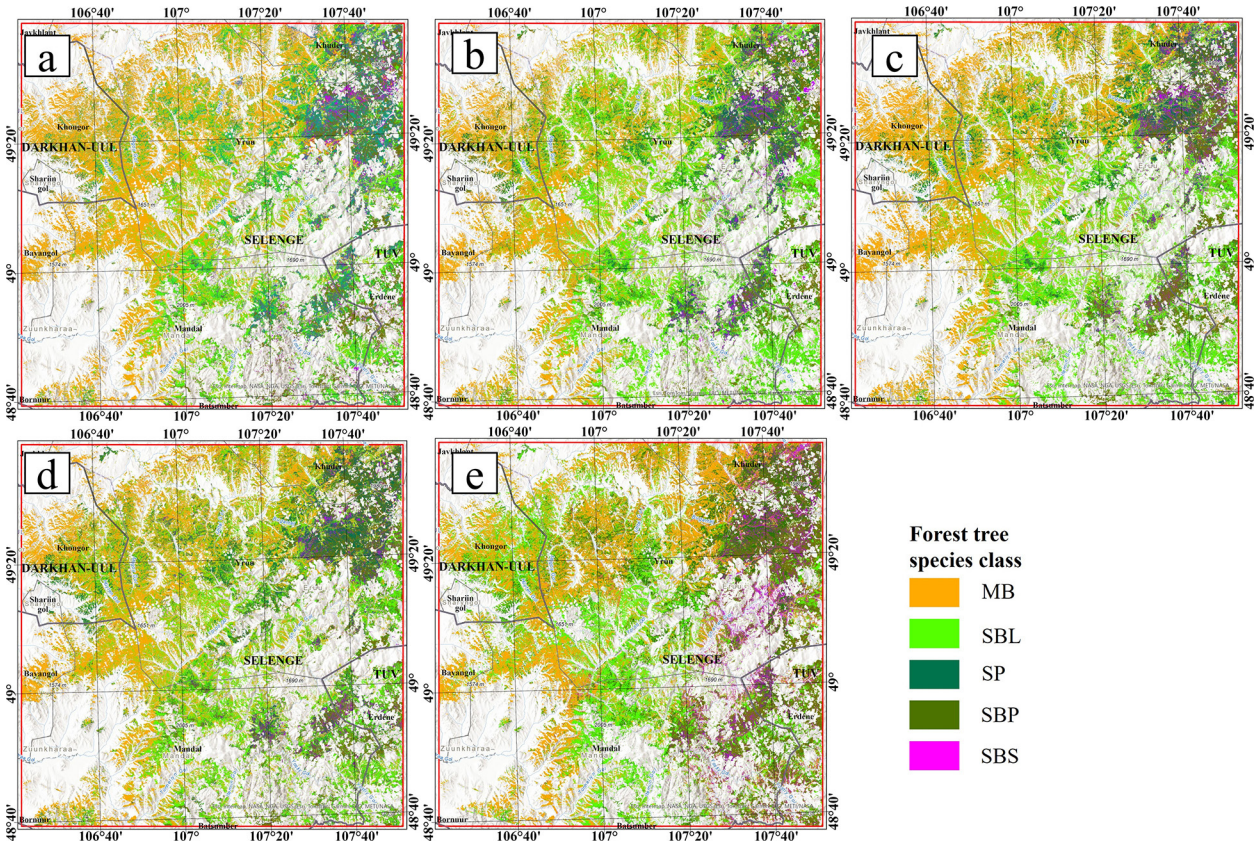

Fig. 8. Forest tree species classification maps for analysed periods: (A) 21.08.2020; (B) 30.08.2021; (C) 30.08.2022; (D) 30.08.2023; (E) 24.08.2024.

The classification maps illustrating annual changes in forest tree species revealed that the alterations were spatially dispersed and did not encompass large contiguous areas (Fig. 9).

Based on the RF classification, MB (*B. platyphylla* Sukaczev) was the dominant tree species in the whole period, consistently covering between 1900 km² and 2188 km², indicating a relatively stable and mature forest presence (Fig. 10, Table 3).

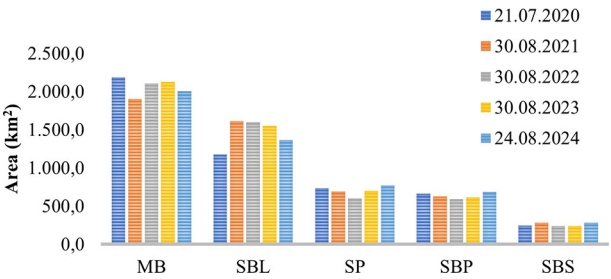

Fig. 10. Dynamic of classified (random forest) forest main tree species classes (single species/total area; km²) on S-2 image (European Space Agency).

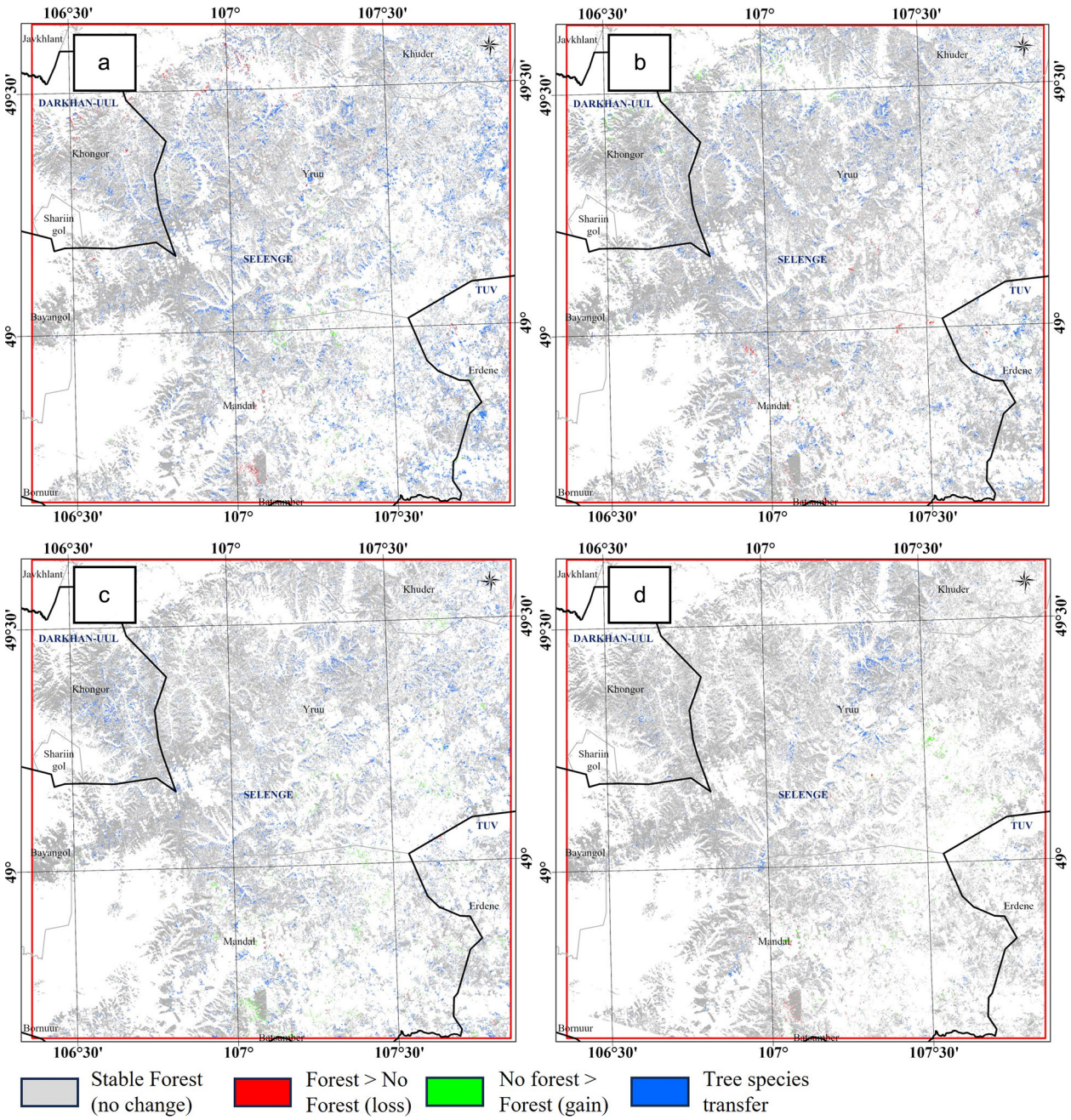

Fig. 9. Change detection map of forest tree species classification: (A) From 2020 to 2021; (B) From 2021 to 2022; (C) From 2022 to 2023; (D) From 2023 to 2024.

Table 3. Classification results using RF approach (bold values represent the total area and overall percentage across all classes).

Class name		Manchurian birch	Siberian larch	Scotch pine	Siberian pine	Siberian spruce	Sum of forest mask	Non-forest	Other	Total (km²)
Sentinel 2 21.07.2020	Area (km²)	2188.5	1178.1	736.0	664.1	243.4	5010.0	1142.3	1233.9	7386.3
	Percentage (%)	29.6	15.9	10.0	9.0	3.3	67.8	15.5	16.7	100.0
Sentinel 2 30.08.2021	Area (km²)	1900.7	1614.3	692.5	626.5	280.8	5114.7	1037.6	1233.9	7386.3
	Percentage (%)	25.7	21.9	9.4	8.5	3.8	69.2	14.0	16.7	100.0
Sentinel 2 30.08.2022	Area (km²)	2107.1	1600.3	602.4	589.7	243.0	5142.4	1009.9	1233.9	7386.3
	Percentage (%)	28.5	21.7	8.2	8.0	3.3	69.6	13.7	16.7	100.0
Sentinel 2 30.08.2023	Area (km²)	2127.3	1555.1	699.0	612.5	241.7	5235.5	9168	1233.9	7386.3
	Percentage (%)	28.8	21.1	9.5	8.3	3.3	70.9	12.4	16.7	100.0
Sentinel 2 24.08.2024	Area (km²)	2008.0	1367.6	769.6	685.1	281.0	5111.3	1041.1	1233.9	7386.3
	Percentage (%)	27.2	18.5	10.4	9.3	3.8	69.2	14.1	16.7	100.0

SBL (*L. sibirica* Ledeb.) ranked as second, with its area fluctuating significantly, from 1178.1 km² (in July 2020), peaking at 1614.3 km² (August 2021), then declining to 1367.6 km² (August 2024). These fluctuations may be related to the seasonal phenological changes of larch, particularly its distinctive needle coloration.

SBP (*P. sibirica* Ledeb.) exhibited minor fluctuations, from 664.1 km² (9.0%) in 2020 to 626.5 km² (8.5%) in 2021, then 589.7 km² (8.0%) in 2022, 612.5 km² (8.3%) in 2023 and 685.1 km² (9.3%) in 2024.

The area of SP (*P. sylvestris* L.) fluctuated over the 5 years. It covered 736.0 km² (10.0%) in 2020, decreased to 692.5 km² (9.4%) in 2021 and 602.4 km² (8.2%) in 2022, then increased to 699.0 km² (9.5%) in 2023 and 769.6 km² (10.4%) in 2024.

SBS (*P. obovata* Ledeb.) maintained relatively stable coverage, ranging from 243.4 km² (3.3%) in 2020 to 280.8 km² (3.8%) in 2021, decreasing slightly to 243.0 km² (3.3%) in 2022, 241.7 km² (3.3%) in 2023 and increasing again to 281.0 km² (3.8%) in 2024 (Table 2). These fluctuations may have been influenced by the mixed forest structure, interspecific competition, and the specific characteristics of natural regeneration in coniferous stands. Furthermore, the temporal difference in data collection – carried out in July 2020 and in August during 2021–2024 – may have contributed to the observed changes due to differences in growth stages, crown density of deciduous species and spectral variations in remote sensing data.

Classification validation

The comprehensive validation of forest tree species classification demonstrates consistently exceptional performance across all evaluated metrics (Table 4). OA remained remarkably high throughout the study period (2020–2024), ranging from 0.939 to a high 0.962, with peak performance observed in the S-2 (July 21, 2021) dataset, achieving near-perfect accuracy and $\kappa = 0.962$.

MB (*B. platyphylla* Sukaczev) consistently shows excellent and stable performance, with sensitivity and specificity generally >0.991 and a slight dip in specificity to 0.984 in 2024, reflecting its distinct canopy and leaf morphology (Thenkabail et al. 2010). SBL (*L. sibirica* Ledeb.) exhibits improving sensitivity from 0.914 in 2020 to 0.942 in 2022 but lower specificity, which dropped in 2021 and remained at lower values, suggesting better detection at the expense of occasional misclassification likely due to needle senescence (Saarinen et al. 2018). SP (*P. sylvestris* L.) maintains consistently high sensitivity and specificity, with specificity reaching a perfect 1.000 in 2021, indicating zero false positives, reflecting the robustness of the RF classifier. SBP (*P. sibirica* Ledeb.) demonstrates high sensitivity and specificity throughout, with a small drop in specificity from 2020 to 2023, followed by its increase in 2024, likely influenced by environmental factors such as canopy shadow or moisture variation (Fassnacht et al. 2016). SBS (*P. obovata* Ledeb.) shows the highest specificity but the lowest and most variable sensitivity, falling

Table 4. Classification validation metrics.

Metric	Range	Interpretation
Accuracy	0.939–0.962	All pixels were classified correctly, showing that the overall performance of the model is very reliable.
Kappa	0.924–0.949	Demonstrates very strong agreement beyond chance, which confirms the consistency and reliability of the classification results
P-value	< 2.2e-16	The findings are extremely statistically significant.
Sensitivity (high class)	0.963–0.980	The model is highly effective in detecting the actual presence of species in these categories.
Sensitivity (low class)	0.867–0.917	Slightly lower sensitivity for species like Spruce, meaning it's harder to correctly identify them.
Specificity	0.975–0.997	Very high species are rarely misclassified as each other.
F1-score	0.935–0.952	Demonstrating excellent performance and a strong balance between precision and recall.

to 0.867 in 2023, indicating a conservative model that avoids false positives but frequently misses true Spruce stands due to spectral similarity with other conifers (Maxwell et al. 2018).

Based on the data from 2020 to 2022, the classification model demonstrate strong performance for non-forest areas and SBS (*P. obovata* Ledeb.), with consistently high accuracy scores. However, it demonstrates significant confusion between SP (*P. sylvestris* L.), SBP (*P. sibirica* Ledeb.) and SBL (*L. sibirica* Ledeb.) classes across all years. The model shows improvement in MB (*B. platyphylla* Sukaczev) classification over time, with misclassification rates decreasing from 501 in 2020 to 264 in 2022 when confused with SBS (*P. obovata* Ledeb.) (Fig. 11).

Comparison of S-2 classification results with the traditional forest inventory from 2019

A comparative analysis of the 2019 forest inventory and S-2 classifications from July 2020

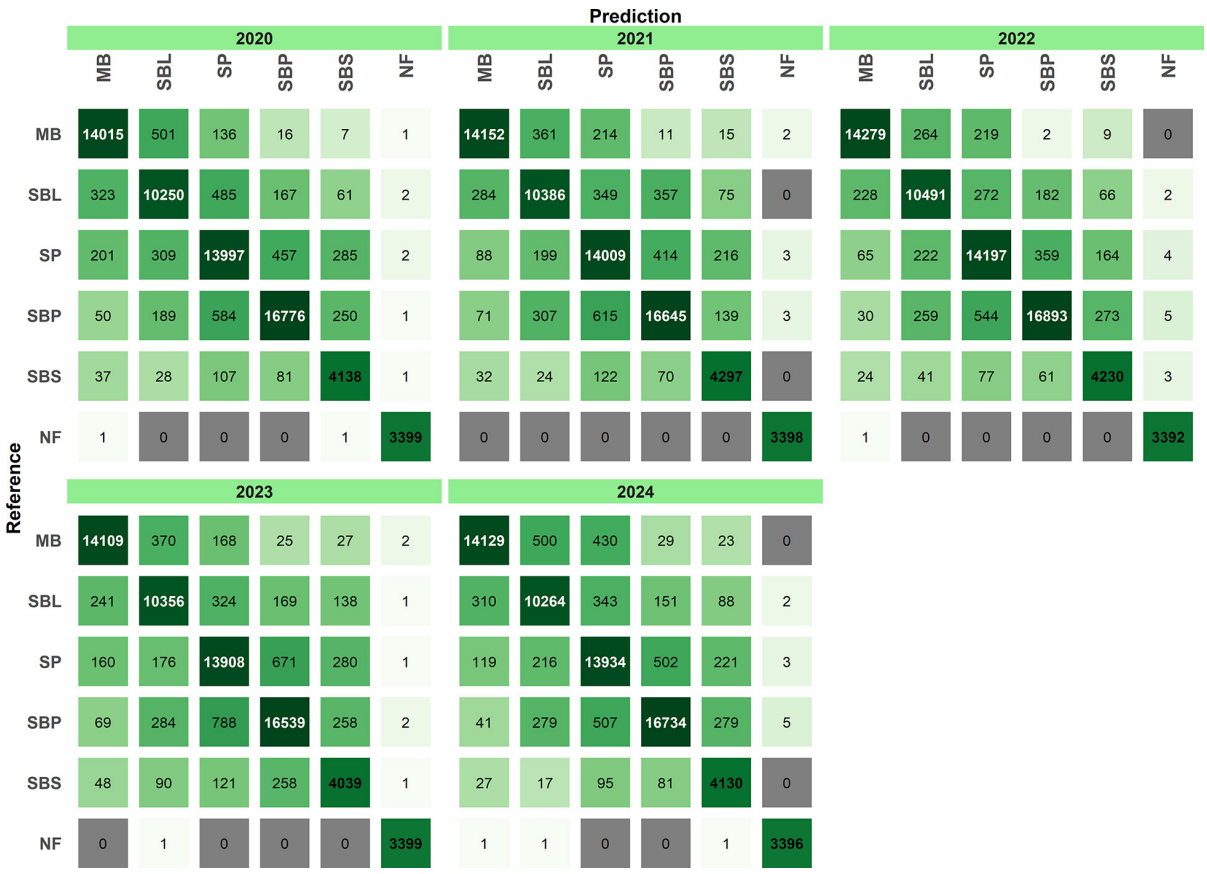

Fig. 11. Confusion matrices for forest type classification (2020–2024).

Table 5. Results of S-2 classification vs. forest inventory data (bold values represent the total area and overall percentage across all classes).

Class	Forest inventory map (2019)		S-2 21/07/2020		Difference		S-2 24/08/2024		Difference	
	km²	%	km²	%	km²	%	km²	%	km²	%
Manchurian birch	2773.9	53.8	2188.5	43.7	−585.4	−21.1	2008.0	39.3	−765.9	−27.6
Siberian larch	912.3	17.7	1178.1	23.5	265.8	29.1	1367.6	26.8	455.3	49.9
Scotch pine	902.7	17.5	735.9	14.7	−166.8	−18.5	769.6	15.1	−133.1	−14.7
Siberian pine	517.4	10.0	664.1	13.3	146.7	28.4	685.1	13.4	167.7	32.4
Siberian spruce	50.9	1.0	243.4	4.9	192.5	378.2	281.0	5.5	230.1	452.1
Total	5157.2	100.0	5010.0	100.0			5111.3	100.0		

and August 2024 reveals substantial shifts in forest composition more than 5 years (Table 5). MB (*B. platyphylla* Sukaczev) declined from 2773.9 km² (53.8%) in 2019 to 2188.5 km² (43.7%) in 2020 and 2008 km² (39.3%) in 2024, a total loss of 765.9 km² (27.6%). SBL (*L. sibirica* Ledeb.) increased from 912.3 km² (17.7%) to 1178.1 km² (23.5%) in 2020 and 1367.6 km² (26.8%) in 2024 (>49.9%), while SBP (*P. sibirica* Ledeb.) grew from 517.4 km² (10.0%) to 685.1 km² (13.4%), a 32.4% increase. SP (*P. sylvestris* L.) remained relatively stable, with minor fluctuations from 902.7 km² (17.5%) to 769.6 km² (15.1%). The most difference occurred in SBS (*P. obovata* Ledeb.), rising from 50.9 km² (1.0%) to 281.0 km² (5.5%), a 452.1% increase, likely reflecting underestimation in the 2019 inventory or classifier confusion. Overall, this considerable discrepancy may be attributable to differences between forest inventory mapping methodologies and remote sensing approaches, as well as to deficiencies in the updating of forest inventory maps.

Discussion

This study highlights the efficacy of using multi-temporal Sentinel-2 (S-2) imagery with the RF algorithm for precise forest tree species classification in Mongolia's boreal regions. The achieved OA of 96.19% and a kappa coefficient of 0.949 align with recent findings using S-2 time series in complex forest environments (Liu et al. 2024). However, discrepancies with the 2019 Forest Inventory data – such as overestimation of SBS (*P. obovata* Ledeb.) and SBL (*L. sibirica* Ledeb.), and underestimation of MB (*B. platyphylla* Sukaczev) – highlight limitations inherent to both field-based mapping and satellite image classification. These inconsistencies likely result from spectral similarity among coniferous species, mixed forest compositions and the absence of ecological or morphometric variables (Dulamsuren et al. 2010a, b, Karthigesu et al. 2025).

The findings corroborate earlier studies in Mongolia (Amarsaikhan et al. 2012, Munkh-Erdene et al. 2018), where classification accuracies of 90–91% were reported using Landsat and ALOS PALSAR data. The higher accuracy in the current study can be attributed to the richer multi-temporal dataset, optimised sampling strategies and the application of ML algorithms (Grabska-Szwagrzyk et al. 2024).

Spectral confusion among coniferous species, particularly between SBS (*P. obovata* Ledeb.) and other evergreen conifers, remains a significant challenge due to overlapping canopy reflectance (Ban et al. 2020, Franklin et al. 2003). The current classification framework did not incorporate morphometric or ecological variables, such as altitude, slope or aspect, which are known to influence species distribution in Mongolia's forest landscapes. Incorporating these variables could further enhance classification accuracy (Erdenebaatar and Damdinsuren 2020).

The conventional forest inventory methodology in Mongolia remains outdated relative to international standards, relying heavily on labour-intensive, time-consuming field measurements (FAO 2005). Insufficient integration of remote sensing, such as Sentinel-2 imagery, limits the detection of forest dynamics, degradation and regeneration (Hansen et al. 2013, Reiche et al. 2016). The combination of multi-temporal S-2 imagery, RF classification and potential integration of NDVI-based phenology (Grabska-Szwagrzyk et al. 2024) provides a scalable and replicable framework for modernising Mongolia's forest inventory system. Such approaches can enhance the detection of mixed forest compositions, improve

classification of spectrally similar species, and support sustainable forest management under changing environmental conditions.

While preparing the manuscript, authors calculated the NDVI index and used it as an explanatory variable. However, it transpired that the RF algorithm produced OA values that were lower (OA = 0.921) than those obtained without using the NDVI index in the predictive model (OA = 0.995). The authors were therefore discouraged from using the NDVI index, which is commonly used in studies. Furthermore, calculating and implementing it as an additional variable in the model prolonged the data processing time.

To improve classification, particularly for SBS (*P. obovata* Ledeb.), future research should integrate airborne laser scanning (ALS) LiDAR or UAV (Unmanned Aerial Vehicle)-based data (Zhong et al. 2022), and very-HR commercial satellite imagery, such as Planet SuperDove or Aleph Satellogic (WV-3/Legion Maxar) (Duncanson et al. 2021). Multi-temporal Sentinel-2 time series, combined with vegetation indices such as NDVI, EVI (Enhanced Vegetation Index), or MTCI (MERIS Terrestrial Chlorophyll Index), provide valuable insights into phenological patterns and could improve species-level discrimination (Grabska-Szwagrzyk et al. 2024).

High accuracy and kappa scores were achieved; however, uncertainties remain due to limited HR reference data and the selection of homogeneous test areas, which may inflate results (Lechner et al. 2020). Yearly variations in species estimates further reflect the challenges of spectral and temporal variability (Lu, Weng 2007). Expanding and diversifying ground-truth datasets will improve model robustness and reliability.

Conclusions

This study confirms that ML, particularly the RF algorithm, applied to Sentinel-2 imageries, enables rapid and accurate forest species classification in boreal regions such as northern Mongolia. Across the five dominant species, the approach achieved an OA of up to 96.19% and kappa values approaching 0.949.

Nonetheless, these performance metrics likely represent an upper bound of true accuracy. Validation data were deliberately selected from homogeneous, representative forest stands – conditions that inherently reduce classification difficulty. The lack of comprehensive, HR reference datasets across more heterogeneous forest mosaics introduces uncertainty, which is reflected in the substantial interannual variability observed in classified areas. Despite these caveats, the approach represents a significant advancement over earlier Mongolian studies, which typically reported accuracies near 90%.

In practical terms, this research offers a scalable and cost-effective tool for operational forest monitoring in Mongolia, supporting management, restoration and climate policy initiatives. However, further improvements are essential. These include incorporating morphometric and ecological layers, using higher-resolution commercial imagery where feasible, expanding field data collection using GNSS (Global Navigation Satellite Systems) or UAV platforms, and exploring more advanced classification methods such as deep learning. This study represents a significant advancement in remote sensing-based forest classification and provides well-defined avenues for further methodological improvement.

Acknowledgements

The research was financially supported by the Rector's grant under the research at the Doctoral School of University of Agriculture in Krakow. We would also like to thank the Editor and the reviewers for their valuable comments and suggestions, which helped improve this paper.

Author's contribution

E.B.: conceptualisation, validation, formal analysis, investigation, data curation, writing – original draft, writing – review & editing, visualisation; P.W.: supervision, conceptualisation, writing – review & editing, investigation, project administration; W.K.: conceptualisation, writing – review & editing, investigation, data curation.

Conflict of interest statement

The authors declare that they have no known competing financial interests or personal relationships that could have appeared to influence the work reported in this paper.

References

Amarsaikhan D., Saandar M., Battsengel V., Amarjargal S., 2012. Forest resources study in Mongolia using advanced spatial technologies. *The International Archives of the Photogrammetry, Remote Sensing and Spatial Information Sciences* XXXIX-B7: 257–262. DOI 10.5194/isprsarchives-xxxix-b7-257-2012.

Ban Y., Zhang P., Nascetti A., Bevington A.R., Wulder M.A., 2020. Near real-time wildfire progression monitoring with Sentinel-1 SAR time series and deep learning. *Scientific Reports* 10(1): 1–15. DOI 10.1038/s41598-019-56967-x.

Belgiu M., Drăguț L., 2016. Random forest in remote sensing: A review of applications and future directions. *ISPRS Journal of Photogrammetry and Remote Sensing* 114: 24–31. DOI 10.1016/j.isprsjprs.2016.01.011.

Blickensdörfer L., Oehmichen K., Pflugmacher D., Kleinschmit B., Hostert P., 2024. National tree species mapping using Sentinel-1/2 time series and German National Forest Inventory data. *Remote Sensing of Environment* 304: 114069. DOI 10.1016/j.rse.2024.114069.

Breiman L., 2001. Random forest. *Machine Learning* 45: 5–32. DOI 10.1023/A:1010933404324.

Congalton R.G., Green K., 2019. Assessing the Accuracy of Remotely Sensed Data, Assessing the Accuracy of Remotely Sensed Data. CRC Press. DOI 10.1201/9780429052729.

Drusch M., Del Bello U., Carlier S., Colin O., Fernandez V., Gascon F., Hoersch B., Isola C., Laberinti P., Martimort P., Meygret A., Spoto F., Sy O., Marchese F., Bargellini P., 2012. Sentinel-2: ESA's optical high-resolution mission for GMES operational services. *Remote Sensing of Environment* 120: 25–36. DOI 10.1016/j.rse.2011.11.026.

Dulamsuren C., Hauck M., Khishigjargal M., Leuschner H.H., Leuschner C., 2010a. Diverging climate trends in Mongolian taiga forests influence growth and regeneration of *Larix sibirica*. *Oecologia* 163(4): 1091–1102. DOI 10.1007/s00442-010-1689-y.

Dulamsuren C., Hauck M., Leuschner C., 2010b. Recent drought stress leads to growth reductions in *Larix sibirica* in the Western Khentey, Mongolia. *Global Change Biology* 16(11): 3024–3035. DOI 10.1111/j.1365-2486.2009.02147.x.

Duncanson L., Armston J., Disney M., Avitabile V., Barbier N., Calders K., Carter S., Chave J., Herold M., MacBean N., McRoberts R., Minor D., Paul K., Réjou-Méchain M., Roxburgh S., Williams M., Albinet C., Baker T., Bartholomeus H., Bastin J.F., Coomes D., Crowther T., Davies S., de Bruin S., De Kauwe M., Domke G., Dubayah R., Falkowski M., Fatoyinbo L., Goetz S., Jantz P., Jonckheere I., Jucker T., Kay H., Kellner J., Labriere N., Lucas R., Mitchard E., Morsdorf F., Naesset E., Park T., Phillips O.L., Ploton P., Puliti S., Quegan S., Saatchi S., Schaaf C., Schepaschenko D., Scipal K., Stovall A., Thiel C., Wulder M.A., Camacho F., Nickeson J., Román M., Margolis H., 2022. Aboveground woody biomass product validation good practices protocol, CEOS Land Product Validation Subgroup. pp: 236. DOI 10.5067/doc/ceoswgcv/lpv/agb.001.

Erdenebaatar N., Damdinsuren A., 2020. Geographical analysis of forest types based on a digital elevation model generated from synthetic aperture radar. *Proceedings of the Mongolian Academy of Sciences* 60(4): 43–54. DOI 10.5564/pmas.v60i4.1504.

European Space Agency, 2024. Sentinel-2. Colour vision for Copernicus. Online: esa.int/Applications/Observing_the_Earth/Copernicus/Sentinel-2. (Accessed: 2023-2025).

FAO [Food and Agriculture Organization], 2021. *Voluntary guidelines on national forest monitoring*.

FAO [Food and Agriculture Organization], 2005. *Mongolia: Forest Resources*. Online: fao.org/4/w8302e/w8302e05.htm.

Fassnacht F.E., Latifi H., Stereńczak K., Modzelewska A., Lefsky M., Waser L.T., Straub C., Ghosh A., 2016. Review of studies on tree species classification from remotely sensed data. *Remote Sensing of Environment* 186: 64–87. DOI 10.1016/j.rse.2016.08.013.

Franklin, S.E., Phinn, S.R., Woodcock, C.E., 2003. Remote Sensing of Forest Environments: Concepts and Case Studies. Springer Science & Business Media. xiv, 519 pp. DOI 10.1007/978-1-4615-0306-4.

Galtbayar S., Myagmarsuren A., Munkhbat B., Tsedev-Ish O., Ulziibaatar M., Gankhuyag U., 2022. Determining variables of social, economic, and ecological vulnerability to climate change. *Mongolian Journal of Geography and Geoecology* 59(43): 30–42. DOI 10.5564/mjgg.v59i43.2510.

Global Forest Watch, 2024. Online: globalforestwatch.org/ (Accessed: 2023-2025).

Mongolian Forest Inventory, 2019. Map (Accessed: 2023).

Grabska-Szwagrzyk E., Tiede D., Sudmanns M., Kozak J., 2024. Map of forest tree species for Poland based on Sentinel-2 data. *Earth System Science Data* 16(6): 2877–2891. DOI 10.5194/essd-16-2877-2024.

Grabska-Szwagrzyk E., Tymińska-Czabańska L., 2024. Sentinel-2 time series: A promising tool in monitoring temperate species spring phenology. *Forestry* 97(2): 267–281. DOI 10.1093/forestry/cpad039.

Hansen M.C., Potapov P.V., Moore R., Hancher M., Turubanova S.A., Tyukavina A., Thau D., Stehman S.V., Goetz S.J., Loveland T.R., Kommareddy A., Egorov A., Chini L., Justice C.O., Townshend J.R., 2013. High-resolution global maps of 21st-century forest cover change. *Science* 342(6160): 850–853. DOI 10.1126/science.1244693.

Immitzer M., Vuolo F., Atzberger C., 2016. First experience with Sentinel-2 data for crop and tree species classifications in Central Europe. *Remote Sensing* 8(3): 166. DOI 10.3390/rs8030166.

Jugder D., Gantsetseg B., Davaanyam E., Shinoda M., 2018. Developing a soil erodibility map across Mongolia. *Natural Hazards* 92(Suppl 1): 71–94. DOI 10.1007/s11069-018-3409-6.

Karthigesu J., Owari T., Tsuyuki S., Hiroshima T., 2025. Improving the individual tree parameters estimation of a complex mixed conifer – Broadleaf forest using a combination of structural, textural, and spectral metrics derived from unmanned aerial vehicle RGB and multispectral imagery. *Geomatics* 5(1): 12. DOI 10.3390/geomatics5010012.

Lapin K., Oettel J., Braun M., H.K. (ed.)., 2025 *Ecological Connectivity of Forest Ecosystems*, *Springer*. DOI 10.1007/978-3-031-82206-3.

Keenan R.J., Reams G.A., Achard F., de Freitas J.V., Grainger A., Lindquist E., 2015. Dynamics of global forest area: Results from the FAO Global Forest Resources Assessment 2015. *Forest Ecology and Management* 352: 9–20. DOI 10.1016/j.foreco.2015.06.014.

Lechner A.M., Foody G.M., Boyd D.S., 2020. Applications in remote sensing to forest ecology and management. *One Earth* 2(5): 405–412. DOI 10.1016/j.oneear.2020.05.001.

Liu P., Chunying R., Zongming W., Mingming J., Wensen Y., Huixin R., Chenzhen X., 2024. Evaluating the potential of

Sentinel-2 time series imagery and machine learning for tree species classification in a mountainous forest. *Remote Sensing* 16(2): 293. DOI 10.3390/rs16020293.

Lugten G., 2020. Food and agriculture organization. *The International Journal of Marine and Coastal Law* 23(4): 761–767. DOI 10.1163/157180808X353939.

Lu D., Weng Q., 2007. A survey of image classification methods and techniques for improving classification performance. *International Journal of Remote Sensing* 28(5): 823–870. DOI 10.1080/01431160600746456.

Maxwell A.E., Warner T.A., Fang F., 2018. Implementation of machine-learning classification in remote sensing: An applied review. *International Journal of Remote Sensing* 39(9): 2784–2817. DOI 10.1080/01431161.2018.1433343.

Ming H., Yanzhu D., Jianguang Z., Yong Z., 2016. A topological enabled three-dimensional model based on constructive solid geometry and boundary representation. *Cluster Computing* 19(4): 2027–2037. DOI 10.1007/s10586-016-0634-1.

Ministry of Environment and Green Development, 2015. *Forest policy of Mongolia*. (Accessed: 2023).

Ministry of Environment and Tourism, 2021. *National campaign for planting one billion trees by 2030*. (Accessed: 2023).

Mongolian Environmental Database, 2025. *Geoinformation database*. Online: eic.mn/ (Accessed: 2025).

Munkh-Erdene A., et al., 2018. Applications of optical and radar images for forest resources study in Mongolia. *Proceedings – 39th Asian Conference on Remote Sensing: Remote Sensing Enabling Prosperity*. ACRS 2018.

National Statistics Office of Mongolia, 2025. *Mongolian statistical information service*. Online: www.1212.mn. (Accessed: 2023-2025).

Norovsuren B., Mart Z., Natsagdorj E., Altanchimeg T., 2023. Developing a multi-variable forest fire risk model and fire risk zone mapping. *The International Archives of the Photogrammetry, Remote Sensing and Spatial Information Sciences* XLVIII-1/W2-2023: 1485–1490. DOI 10.5194/isprs-archives-XLVIII-1-W2-2023-1485-2023.

Ochirbat B., Purevsuren O., Manaljav S., 2022. Soil erosion study of the Gobi Desert region using the cesium-137 isotope method. *Mongolian Journal of Geography and Geoecology* 59(43): 74–83. DOI 10.5564/mjgg.v59i43.2514.

Persson M., Lindberg E., Reese H., 2018. Tree species classification with multi-temporal Sentinel-2 data. *Remote Sensing* 10(11): 1–17. DOI 10.3390/rs10111794.

Reiche J., Lucas R., Mitchell A.L., Verbesselt J., Hoekman D.H., Haarpaintner J., Kellndorfer J.M., Rosenqvist A., Lehmann E.A., Woodcock C.E., Seifert F.M., Herold M., 2016. Combining satellite data for better tropical forest monitoring. *Nature Climate Change* 6: 120–122. DOI 10.1038/nclimate2919.

Saarinen N., Vastaranta M., Näsi R., Rosnell T., Hakala T., Honkavaara E., Wulder M.A., Luoma V., Tommaselli A.M.G., Imai N.N., Ribeiro E.A.W., Guimarães R.B., Holopainen M., Hyyppä J., 2018. Assessing biodiversity in boreal forests with UAV-based photogrammetric point clouds and hyperspectral imaging. *Remote Sensing* 10(2): 338. DOI 10.3390/rs10020338.

Senez-Gagnon F., Thiffault E., Paré D., Achim A., Bergeron Y., 2018. Dynamics of detrital carbon pools following harvesting of a humid eastern Canadian balsam fir boreal forest. *Forest Ecology and Management* 430: 33–42. DOI 10.1016/j.foreco.2018.07.044.

Silva B.L.C., Souza F.C., Ferreira K.R., Queiroz G.R., Santos L.A., 2022. Spatiotemporal segmentation of satellite image time series using self-organizing map. *ISPRS Annals of the Photogrammetry, Remote Sensing and Spatial Information Sciences* 5(3): 255–261. DOI 10.5194/isprs-Annals-V-3-2022-255-2022.

Thenkabail P.S., 2010. Global croplands and their importance for water and food security in the twenty-first century: Towards an ever green revolution that combines a second green revolution with a blue revolution. *Remote Sensing* 2(9): 2305–2312. DOI 10.3390/rs2092305.

United Nations, 2015. UN General Assembly, Transforming our world: The 2030 agenda for sustainable development. Resolution adopted by the General Assembly on 25 September 2015. Vol. 16301. 1–35. Online: refworld.org/docid/57b6e3e44.html.

UNECE (2024) *Boreal forests: A global treasure*. Available at: unece.org.

Zhong H., Lin W., Liu H., Ma N., Liu K., Cao R., Wang T., Ren Z., 2022. Identification of tree species based on the fusion of UAV hyperspectral image and LiDAR data in a coniferous and broad-leaved mixed forest in Northeast China. *Frontiers in Plant Science* 13: 1–17. DOI 10.3389/fpls.2022.964769.